PERGAMON

Journal of Geodynamics 33 (2002) 43–52

JOURNAL OF
GEODYNAMICS

www.elsevier.com/locate/jgeodyn

Validation of fast pre-mission error analysis of the GOCE gradiometry mission by a full gravity field recovery simulation

Nico Sneeuw[a,*], José van den IJssel[b], Radboud Koop[b], Pieter Visser[b], Christian Gerlach[a]

[a]*Institut für Astronomische und Physikalische Geodäsie, TU Munich, Germany*
[b]*Delft Institute for Earth-Oriented Space Research, DEOS, TU Delft, The Netherlands*

Abstract

Spherical harmonic error analysis fully relies on the validity of the a priori observational and stochastic models. In this paper we validate error analysis results of the gradiometer mission GOCE by a full-fledged spherical harmonic coefficient recovery. Both methods (least squares error analysis and full recovery) are based on a semi-analytical approach. The results compare very well in spectral and spatial domains. Thus, it is demonstrated that, besides being fast, the least squares error analysis is a reliable premission error assessment tool. © 2002 Elsevier Science Ltd. All rights reserved.

1. Introduction

The gravity gradiometry satellite mission GOCE (gravity field and steady-state ocean circulation explorer) is the first Earth explorer core mission selected in the Living Planet Programme of the European Space Agency (ESA). GOCE aims for the high-precision and high-resolution recovery of the Earth's gravitational field with an accuracy better than 1–2 mGal (1 mGal $= 10^{-5}$ m/s^2) and the corresponding geoid better than 1 cm. These goals are to be attained at length scales down to 100 km, (cf. ESA, 1999).

To this end GOCE will carry a sensitive gravity gradiometer, measuring the diagonal components (V_{xx}, V_{yy}, V_{zz}) of the gravity gradient tensor. In the measurement bandwidth (MBW) between $5{\cdot}10^{-3}$ and 0.1 Hz the observation requirement on the error power spectral density (PSD) is $3{\cdot}10^{-3}$ E/$\sqrt{\text{Hz}}$ (1 E $= 10^{-9}$ s^{-2}). Below the MBW the gradiometry degrades with $1/f$. Moreover, an on-board GPS receiver will track the satellite's orbit precisely. Due to a drag-free

* Corresponding author.
E-mail address: sneeuw@ucalgary.ca (N. Sneeuw).

0264-3707/02/$ - see front matter © 2002 Elsevier Science Ltd. All rights reserved.
PII: S0264-3707(01)00053-9

system the satellite will follow a gravitational trajectory. The orbit will be near-circular at an approximate height of 250 km and sun-synchronous ($I \approx 96^\circ.5$). GOCE is due for launch in 2004.

Prior to launch several mission scenarios are investigated. Orbit parameters, gradiometer performance, system configuration, effects of attitude and orbit control design, and so on, affect the mission result in terms of geoid or gravity field accuracy. Ideally, these mission scenarios are simulated in an end-to-end simulation, recovering the spherical harmonic (SH) coefficients from simulated gravity gradients, that have been contaminated by one or more of the above effects. Considering the fact that 8 months of mission data would have to be simulated for each scenario, and considering the complexity of gravity field recovery, it becomes clear that end-to-end analysis in this fashion is infeasible at this stage.

Least squares error analysis provides an easy means of investigating the accuracy with which unknown parameters can be estimated from a set of observations, even without an actual experiment carried out, (cf. Sneeuw et al., 1996). It requires a linear model, linking observables to unknowns. Apart from a distinction between brute-force numerical and (semi-)analytical modelling, several modelling options exist, (e.g. Rummel et al., 1993). Our choice here is the *time-wise* approach, in particular the *frequency-domain* variant, as opposed to the *space-wise* approach. The choice for frequency-domain modelling follows from the fact that the input for the stochastic model comes from power spectral densities (PSDs), i.e. spectral error representations. See also (Balmino et al., 1998).

The validity of least squares error analysis fully relies on the quality of the linear model. Particularly the a priori stochastic model deserves special attention. For instance a wrong a priori variance factor scales directly into the output error spectrum σ_{lm}. Therefore, these error spectra have to be validated against the results of a *full gravity field recovery* simulation.

2. Simulation logic

In the course of the GOCE Phase A studies numerous mission scenarios have been simulated by the SID consortium (SID, 2000). The simulation logic is clarified by Fig. 1. Starting from an input gravity field model (K_{lm}, top right corner) an orbit (x) is integrated. Along this orbit gravity gradients (V_{ij}^{in}) are calculated. These are input to the core of the simulator, the gradiometer model (the box containing the word *forward*). Depending on hardware parameters and spacecraft dynamics, contaminated output gravity gradients (V_{ij}^{out}) are generated (by the box containing *backward*). The difference between input and output gradients (ΔV_{ij}, middle lower branch) is a measure of the errors induced by the central gradiometer model.

After Fourier transformation an error power spectral density (PSD) is obtained, which is the basis for the stochastic model. Least squares error analysis basically yields the SH error spectrum (σ_{lm}) and correlations between the coefficients (not denoted here). By further covariance propagation one may obtain a spatial representation of the geoid error (σ_N) and of gravity anomalies ($\sigma_{\Delta g}$).

The bottom right line of processing represents the full gravity field recovery, leading to output SH coefficients (K_{lm}^{out}). The difference between output and input coefficients is called ΔK_{lm}. Validation of the least squares error analysis results against full gravity field recovery is indicated by the dashed line between the bottom right oval boxes. If the difference spectrum compares well to the error spectrum, one can be confident that the stochastic modelling has been correct.

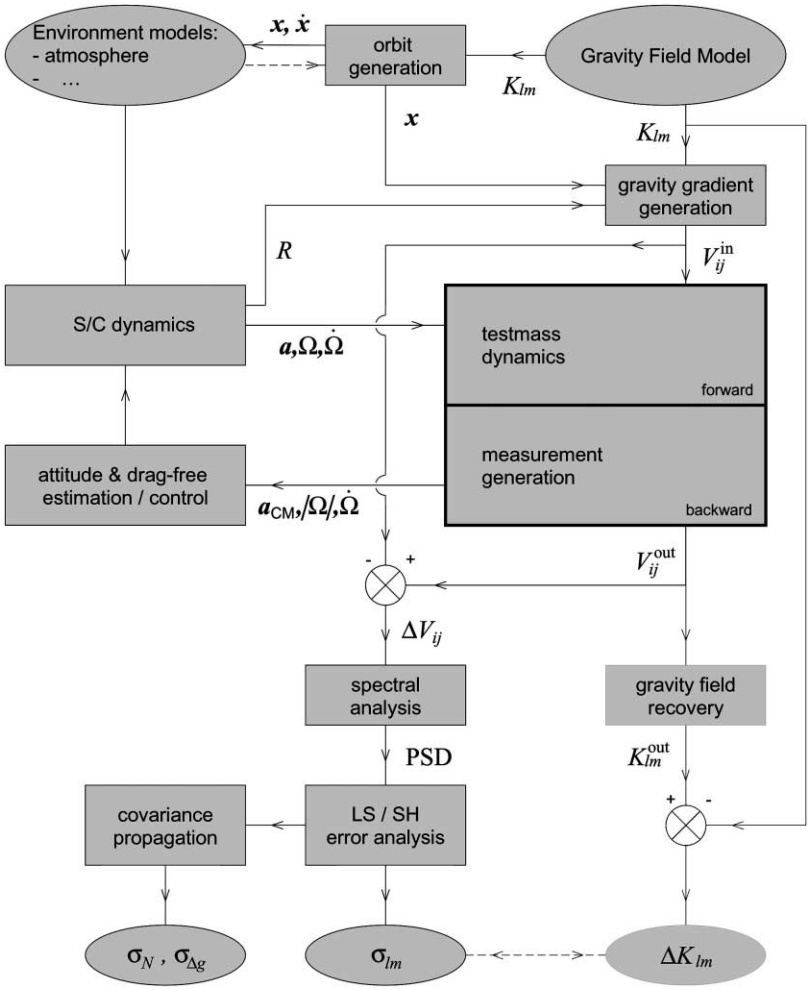

Fig. 1. End-to-end simulation logic.

3. The time-wise frequency-domain linear model

The Earth's gravitational potential is conventionally expressed as a spherical harmonic series, here in complex-valued notation:

$$V(r,\theta,\lambda) = \frac{GM}{r}\sum_{l=0}^{L}\left(\frac{R}{r}\right)^{l}\sum_{m=-l}^{l} K_{lm}\,Y_{lm}(\theta,\lambda). \tag{1}$$

For convenience a band limitation up to maximum degree L is assumed. Furthermore, it is assumed that quantities are fully normalized. If we use the following orbital variables:

$$u = \omega + \nu = \text{argument of latitude}$$

$$\Lambda = \Omega - \mathrm{GAST} = \text{longitude of ascending node}$$

$$\text{with} \qquad \omega = \text{argument of perigee}$$

$$\nu = \text{true anomaly}$$

$$\Omega = \text{right ascension of ascending node}$$

$$\mathrm{GAST} = \text{Greenwich actual sidereal time}$$

the gravitational potential V along the orbit is given by the following two-dimensional Fourier expression, (cf. Sneeuw et al., 1996):

$$V(u, \Lambda) = \sum_{m=-L}^{L} \sum_{k=-L}^{L} A_{mk}^{V} \mathrm{e}^{i(ku+m\Lambda)}. \tag{2}$$

The Fourier coefficients A_{mk}^{V} of the potential are also known as *lumped coefficients,* since they form a linear combination of spherical harmonic coefficients K_{lm}:

$$A_{mk}^{V} = \sum_{l=\max(|m|,|k|)}^{L} H_{lmk}^{V} K_{lm}. \tag{3}$$

This equation provides a mapping from the earth-fixed spherical harmonic spectrum K_{lm} to the along-orbit Fourier spectrum A_{mk}^{V} of the potential. Essential are the *transfer* (or *sensitivity*) coefficients H_{lmk}^{V}:

$$H_{lmk}^{V} = \frac{GM}{r} \left(\frac{R}{r}\right)^{l} F_{lmk}(I). \tag{4}$$

This formulation is similar to the one in (Kaula, 1966), although we use a complex-valued representation and do not develop u and r into a series of eccentricity functions. Eqs. (2)–(4) are exact, but hardly practicable. Due to variations in height and inclination the transfer coefficients would be time-dependent. By introducing the concept of a *nominal orbit* with fixed radius and inclination, Eq. (3) is turned into a time-independent linear system with constant coefficients. If the lumped coefficients are considered as observables—although they are the Fourier spectrum of observables, really—the transfer coefficients constitute the linear model, required for the least squares process.

The lumped coefficient formulation (3) can be generalized now to any functional f of the gravitational potential:

$$f(u, \Lambda) = \sum_{m=-L}^{L} \sum_{k=-L}^{L} A_{mk}^{f} \mathrm{e}^{i(ku+m\Lambda)}, \tag{5}$$

$$A^f_{mk} = \sum_{l=\max(|m|,|k|)}^{L} H^f_{lmk} K_{lm}. \tag{6}$$

Each functional, i.e. observable along the orbit, is determined by its own transfer coefficients H^f_{lmk}. They can be derived from H^V_{lmk} by proper differentiations, in case of gradient tensor components, or by involving an orbit perturbation theory, (e.g. Schrama, 1991 or ESA, 1999). Relevant to the GOCE mission are the transfer coefficients from the box below. For the course of this study only H^{xx}_{lmk}, H^{yy}_{lmk} and H^{zz}_{lmk} are relevant.

$$\begin{aligned}
H^{\Delta x}_{lmk} &= \frac{2(l+1)\beta_{mk} - k\left(\beta^2_{mk}+3\right)}{\beta^2_{mk}\left(\beta^2_{mk}-1\right)} \quad \frac{i}{n^2 r} \quad H^V_{lmk} \\
H^{\Delta y}_{lmk} &= \frac{1}{1-\beta^2_{mk}} \quad \frac{1}{n^2 r} \quad H^*_{lmk} \\
H^{\Delta z}_{lmk} &= \frac{(l+1)\beta_{mk} - 2k}{\beta_{mk}\left(\beta^2_{mk}-1\right)} \quad \frac{1}{n^2 r} \quad H^V_{lmk} \\
H^{xx}_{lmk} &= -\left(k^2+l+1\right)^2 \quad \frac{1}{r^2} \quad H^V_{lmk} \\
H^{yy}_{lmk} &= k^2-(l+1)^2 \quad \frac{1}{r^2} \quad H^V_{lmk} \\
H^{zz}_{lmk} &= (l+1)(l+2) \quad \frac{1}{r^2} \quad H^V_{lmk} \\
H^{xz}_{lmk} &= -ik(l+2) \quad \frac{1}{r^2} \quad H^V_{lmk}
\end{aligned} \tag{7}$$

The coordinate directions pertain to a local co-rotating triad with along-track (x), cross-track (y) and radial (z) axes. The first three terms, Δx, Δy and Δz, refer to orbit perturbations, which can be derived from GPS observations. The latter four terms refer to the gravity gradient tensor components, to be measured by the GOCE gradiometer. The quantity β_{mk} denotes the normalized perturbing frequency, expressed in *cycles per revolution* (CPR): $\beta_{mk} = \left(k\dot{u} + m\dot{\Lambda}\right)/n$ with n the orbit frequency. Eq. (7) reveals that resonance occurs around $\beta_{mk} \in \{-1, 0, 1\}$, i.e. at once per revolution and at DC.

All transfer coefficients are expressed as modulations of the basic transfer coefficients H^V_{lmk}, except for $H^{\Delta y}_{lmk}$. The cross-track transfer coefficient H^*_{lmk} is explained in Rummel et al. (1993). The gradiometry transfer coefficients are seen to be of order $\mathcal{O}(l^2, k^2)$. This quadratic amplification factor is the very reason that gravity gradiometry is the preferred satellite geodetic method for high-resolution gravity field determination.

4. Least squares error analysis

Inspection of Eq. (6) shows that a certain lumped coefficient of order $m=m_1$, $A^f_{m_2k}$ does not have parameters K_{lm} in common with lumped coefficients $A^f_{m_2k}$ of different orders $m=m_2$. If they are also stochastically uncorrelated, the error analysis can be performed for each order m separately, yielding a very efficient algorithm (cf. Koop, 1993).

Suppose all lumped coefficients A^f_{mk} for a specific order m are stored into a vector y. This vector is treated as the vector of observations. Spherical harmonic coefficients K_{lm} for the same order m are stored in a vector x: the vector of unknowns. The transfer coefficients, finally, constitute the design matrix A. The linear model (6) reduces to a simple:

$$y = Ax.$$

To be precise, two linear systems arise for each order m, which is due to the property $F_{lmk}(I)=0$ for l–k odd. Thus the maximum length of x, i.e. the maximum amount of unknowns per block, is $L/2$. At the same time, this is the maximum dimension of the sub-blocks of the normal matrix. For increasing order m, the length of x decreases.

Next, a stochastic model is needed. The variances of the vector y go into the matrix Q_{yy}. This matrix represents measurement precision, mission duration, sampling rate, possible band limitations, and so on (cf. Schrama, 1991). Since our observables are the discrete spectral coefficients A^f_{mk}, the corresponding continuous PSD must be discretized. To this end PSD_{mk}, that is the PSD evaluated at the frequency $k\dot{u}+m\dot{\Lambda}$, is integrated over a tiny bandwidth Δf around it. Δf is the spectral resolution, defined by and inversely proportional to the time-series length or mission duration T. Thus we have:

$$\sigma^2_{mk} = \mathrm{PSD}_{mk}\Delta f = \frac{\mathrm{PSD}_{mk}}{T}. \tag{8}$$

Furthermore, one may want to incorporate a priori information, such as Kaula's rule (signal variance of x) or a pre-existing gravity field error (error variance of x), in order to stabilize the normal matrix inversion. This type of regularization provides some matrix K.

Least squares error analysis basically requires to set up the normal matrix N, block by block. Its inverse (also block-wise) yields the a posteriori variance-covariance matrix of the unknowns:

$$N = A^T Q^{-1}_{yy} A + K \;\Rightarrow\; Q_{xx} = N^{-1}. \tag{9}$$

With multiple observables, each observation type provides its own normal matrix N_i:

$$N = \sum_i N_i = \sum_i A_i^T Q^{-1}_{y_iy_i} A_i + K \;\Rightarrow\; Q_{xx} = N^{-1}. \tag{10}$$

Note that these calculations can take place without any actual observations y being made. In combination with the block-diagonal structure of the normal matrix, this is the reason that least squares error analysis is such a powerful pre-mission assessment tool.

The main diagonal of Q_{xx} represents the a posteriori error variances of the unknowns. Its square root thus gives the a posteriori SH error spectrum σ_{lm}. A more common way of presenting the result is to take the square root of the average variance over all coefficients K_{lm} of the same degree l. This provides an RMS error measure for a coefficient of that specific degree: RMS_l. Of course, covariances between spherical harmonic coefficients have been ignored this way.

The above error representations are spectral. A spatial error representation, i.e. standard deviations and covariance functions of the geoid and of gravity anomalies, are obtained by further error propagations. These computations make use of equations, based on (1). They can be performed block-wise as well and incorporate the full correlation structure per block.

A typical result is the SH error spectrum σ_{lm} (right panel) in Fig. 2. It is based on one of the many case studies from (SID, 2000). The particular case study was based on realistic GOCE error sources concerning drag, misalignment of sensitive axes, and so on. This is not relevant to this study, though. For purposes of comparison with the full recovery results, the maximum degree has been cut off here at $L=180$. At this degree, however, the number of significant digits still lies

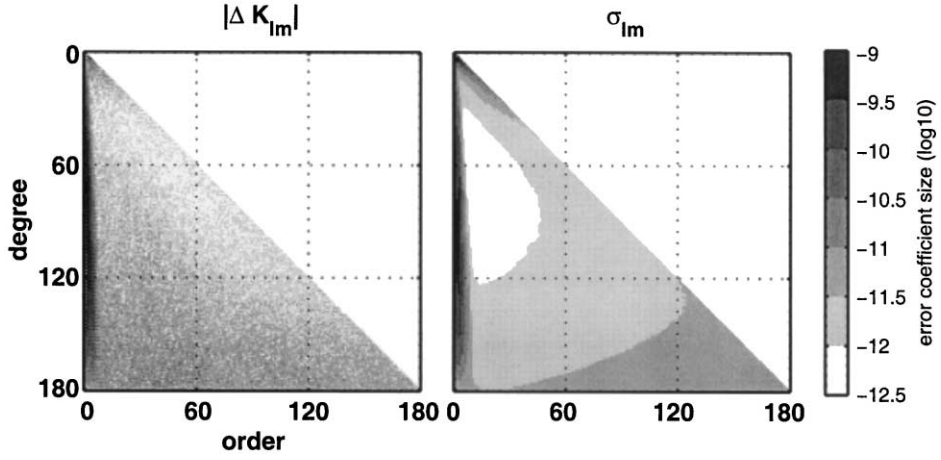

Fig. 2. Comparing spectral difference and SH error spectrum σ_{lm}.

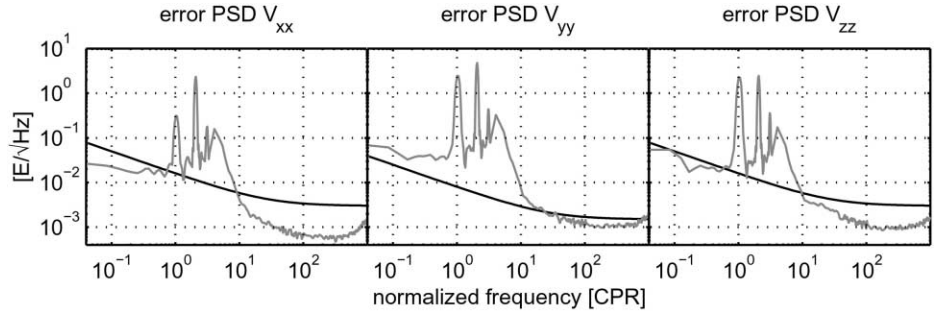

Fig. 3. Simulated (grey) and model (smooth black curves) PSDs.

above 1. The maximum resolution will be attained around degree 300, where the number of significant digits becomes zero, equivalent to a signal-to-noise ratio of 1.

Fig. 2 (right panel) shows that the low order coefficients cannot be determined very well. This is typical for non-polar satellites. The effect is caused by the polar gaps, where effectively no data exist. This is the main reason for applying regularization. In case of GOCE, the spherical radius of these gaps is around 7°. In the propagated geoid errors, cf. Fig. 4 (right), the effect shows up as large geoid errors around the poles.

5. Full gravity field recovery

Whereas least squares error analysis requires the computation of the inverse of the normal matrix N, cf. (9), without using the observations y, full gravity field recovery means to solve the linear model (6) for the spherical harmonic coefficients K_{lm} collected in the vector x from the observations y by means of a least squares estimation procedure. Without any approximations and assumptions on the model and the data, this estimation procedure is a huge computational task when months of data have to be analysed and many coefficients up to a high maximum degree L have to be estimated. However, the block-diagonal structure of the normal matrix described earlier will make the process computationally feasible in view of the required computer time.

Since the block-diagonal structure is obtained only under certain assumptions, the estimation process is performed iteratively whereby in each step updates to the solved parameters x are computed until the solution converges. This iterative, semi-analytical solution scheme, formulated in the time-wise time-domain approach, can be shown to converge to the right solution, see (Klees et al., 2000). It has been implemented and by means of simulation studies it has been shown that the procedure works well within reasonable time constraints (ibid.).

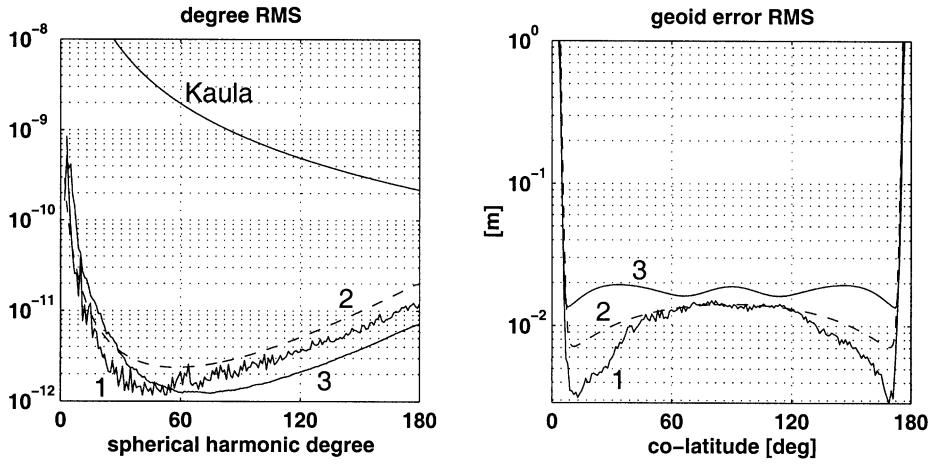

Fig. 4. Left panel: RMS_l results from full coefficient recovery (1) and from least squares analysis using the simulated (3) and model (2) PSDs. Right panel: corresponding longitude-averaged geoid errors $\sigma_N(\theta)$.

In the simulation studies performed so far, a smooth model PSD (see next section) is taken to represent the stochastic properties of the measurements y as they go into the weight matrix Q_{yy}. However, realistic error PSDs as they come out of the simulator (see Fig. 1) may be used instead since the time-wise formulation provides a direct inclusion of the spectral characteristics of the measurement errors without having to apply filtering techniques.

The full recovery experiment presented here included the estimation of the spherical harmonic coefficients up to degree and order 180. Nearly a month of data is required for a solution up to such maximum degree. Gradient data along a 29-days, non-circular, sun-synchronous repeat orbit were simulated for this purpose. Simulated measurement noise corresponding to the expected error behaviour of the GOCE gradiometer was put on the gradient data. Three iterations were necessary to reach the accuracy shown in the figures.

6. Comparison of SH error analysis to full recovery

The validation of the SH error results and those of the full SH coefficient recovery consists of comparing error spectra σ_{lm} to difference spectra ΔK_{lm}, as indicated by the bottom-right dotted line in Fig. 1.

In the 2D spherical harmonic domain the comparison does not seem to be very successful, cf. Fig. 2. The polar gap effect is visible in both triangles. The tendency is for the higher degrees to be worse. Also for the lowest degrees, the grey levels in Fig. 2 (left) are somewhat darker. However, the single ΔK_{lm} are random samples from a given statistical distribution, whereas the σ_{lm} are standard deviations, i.e. statistical averages. Therefore, the ΔK_{lm} should be viewed *on the average*, which is exactly done by the RMS_l quantity, cf. Fig. 4 (left). These 1D error quantities compare very well.

The comparison is complicated by the fact that the stochastic model, as used in the full recovery, is a smooth model PSD, with white noise levels of 3 $\mathrm{mE}/\sqrt{\mathrm{Hz}}$ (V_{xx} and V_{zz}) and 1.5 $\mathrm{mE}/\sqrt{\mathrm{Hz}}$ (V_{yy}), and with $1/f$ increase below a corner frequency of 5mHz ($\approx$ 27 CPR). Therefore the SH error analysis has been run both with the model PSD and with a more realistic PSD as derived from the differences ΔV_{ij}. Apart from the smoothness, Fig. 3 shows that the model PSDs are worse in the MBW. Below the MBW the approximated $1/f$ part is more optimistic than the simulated PSD. The RMS_l curves corresponding to the more realistic PSDs will necessarily be lower than those from the model PSDs, since most gravity field information comes from the MBW. The error level from the deterministic retrieval will be in between. This behaviour is demonstrated in Fig. 4 (left panel) indeed.

The difference between input and output SH coefficients ΔK_{lm} from the full recovery, giving rise to the above spectral error curves in Fig. 4 (left), also causes a spatial difference in geoid and gravity field. The longitude-averaged geoid RMS value can be compared directly to the propagated geoid error $\sigma_N(\theta)$. Also here the full recovery result is compared with simulation results based on the realistic error PSD and on the smoothed model PSD. Fig. 4 (right) clearly demonstrates in the spatial domain the high level of compatibility between the several types of error assessment. The higher geoid error level in case 3, corresponding to the use of the realistic error PSD, is caused by the higher RMS_l for the lowest degrees. This effect would vanish as soon as GPS observations are added.

7. Conclusions

Due to the block-diagonal structure of the normal matrices in the semi-analytical approach, SH error analysis up to high degree and order is feasible with relatively simple computational means. This fact facilitates quick error assessment, with the potential of analyzing many scenarios, investigating the effect of instrument parameters, orbit design, and so on. The only drawback of this otherwise ideal pre-mission assessment tool is the fact that it depends on the validity of the input observation and stochastic model.

Opposed to SH error analysis, a full recovery simulation employs (simulated) data that are based on the unknowns themselves. Thus, after recovery the estimated unknowns can be compared to the input, revealing directly the validity of the simulation. Necessarily, this approach is slower than plain SH error analysis. In the semi-analytical approach, however, this drawback is not too stringent.

The merit of this study is that both approaches have been compared. Most important conclusion from this exercise is the strong agreement between the spectral and spatial error levels from full recovery on the one hand and from SH error analysis on the other hand. Thus the validity of output from spherical harmonic error analyses, as usually employed in mission assessments, is demonstrated.

Acknowledgements

This work has been funded in part under ESA/ESTEC contract No. 12735/98/NL/GD. We are mostly indebted to our colleagues from the SID-Consortium, existing of SRON (Space Research Organization Netherlands), IAPG (Institut für Astronomische und Physikalische Geodäsie) and DEOS (Delft Institute for Earth-Oriented Space Research). The help of Alenia Aerospazio, Italy, is also greatly acknowledged.

References

Balmino, G., Perosanz, F., Rummel, R., Sneeuw, N., Sünkel, H., Woodworth, P., 1998. European Views on Dedicated Gravity Field Missions: GRACE and GOCE, ESA ESD-MAG-REP-CON-001.

ESA, 1999. Gravity Field and Steady-State Ocean Circulation Mission, ESA SP-1233(1).

Kaula, W.M., 1966. Theory of Satellite Geodesy. Blaisdell Publishing, Waltham, MA.

Klees, R., Koop, R., Visser, P., van den IJssel, J., 2000. Fast gravity field recovery from GOCE gravity gradient observations. J. Geodesy 74, 561–571.

Koop, R., 1993. Global Gravity Field Modelling Using Satellite Gravity Gradiometry. Publications on Geodesy, New Series 38, Netherlands Geodetic Commission.

Rummel, R., van Gelderen, M., Koop, R., Schrama, E., Sansò, F., Brovelli, M., Migliaccio, F., Sacerdote, F., 1993. Spherical Harmonic Analysis of Satellite Gradiometry. Publications on Geodesy, New Series 39, Netherlands Geodetic Commission.

Schrama, E.J.O., 1991. Gravity field error analysis: applications of global positioning system receivers and gradiometers on low orbiting platforms. J. Geophys. Res. 96 (B12), 20041–20051.

SID, 2000. GOCE End to End Performance Analysis, ESA/ESTEC contract No. 12735/98/NL/GD.

Sneeuw, N.J., Koop, R.J.J., Schrama, E.J.O., 1996. Global gravity field error analysis for the STEP geodesy co-experiment using GPS and gradient observations. In: Reinhard, R. (Ed.), STEP, Testing the Equivalence Principle in Space, ESA WPP-115.